AGU PUBLICATIONS

Geophysical Research Letters

RESEARCH LETTER
10.1002/2014GL060732

**Key Points:**
- Demonstrate the influence of stream hydromorphology on nitrous oxide emissions
- Estimate the role of rivers in nitrous oxide emissions at the network scale
- Provide an upscaling method for stream biogeochemical processes

**Correspondence to:**
A. Marzadri,
alessandra.marzadri@ing.unitn.it

**Citation:**
Marzadri, A., D. Tonina, A. Bellin, and J. L. Tank (2014), A hydrologic model demonstrates nitrous oxide emissions depend on streambed morphology, *Geophys. Res. Lett.*, *41*, doi:10.1002/2014GL060732.

Received 4 JUN 2014
Accepted 18 JUL 2014
Accepted article online 23 JUL 2014

# A hydrologic model demonstrates nitrous oxide emissions depend on streambed morphology

**A. Marzadri[1,2], D. Tonina[2], A. Bellin[1], and J. L. Tank[3]**

[1]Department of Civil, Environmental and Mechanical Engineering, University of Trento, Trento, Italy, [2]Center for Ecohydraulics Research, University of Idaho, Boise, Idaho, USA, [3]Department of Biological Sciences, University of Notre Dame, Notre Dame, Indiana, USA

**Abstract** Rivers are hot spots of nitrous oxide ($N_2O$) emissions due to denitrification. Although the key role of rivers in transforming reactive inorganic nitrogen is widely recognized, the recent estimates of $N_2O$ emissions by the Intergovernmental Panel on Climate Change (IPCC) may be largely underestimated. This denotes a lack of reliable and robust methodologies to upscale denitrification, and other biogeochemical processes, from the local to the network scale. Here we demonstrate that stream hydromorphology strongly influences $N_2O$ emissions. We provide an integrative methodology for upscaling local biogeochemical processes to the catchment scale with a Damköhler number, which accounts for the complex interplay between stream hydromorphology and biogeochemical characteristics of streambed sediments. Application of this theoretical framework to the large data set collected as part of the second Lotic Intersite Nitrogen eXperiment (LINXII) demonstrates that stream morphology is a key factor controlling emissions of $N_2O$ from streams.

## 1. Introduction

Anthropogenic activities, primarily for food and energy production, have altered the global nitrogen (N) cycle and increased bioavailability of dissolved inorganic nitrogen (i.e., ammonium and nitrate) in many streams and rivers worldwide [*Alexander et al.*, 2000; *Galloway et al.*, 2003, 2004]. Excess inorganic N is often associated with negative consequences including eutrophication of water bodies, periods of water column hypoxia, and increases in stream emissions of nitrous oxide ($N_2O$) as byproduct of microbially mediated denitrification [*Beaulieu et al.*, 2011; *Vitousek et al.*, 1997; *Peterson et al.*, 2001; *Syakila and Kroeze*, 2012; *Rosamond et al.*, 2012]. The sharp increase in the emission rate of $N_2O$ contributes to climate change through stratospheric ozone destruction [*Syakila and Kroeze*, 2012; *Rosamond et al.*, 2012]. Intergovernmental Panel on Climate Change reports that concentrations of atmospheric $N_2O$ have increased by 20% compared to preindustrial times, with agricultural practices and industrial activities being the main sources of emissions [*Kroeze et al.*, 1999]. Approximately 10% of the increase is believed to originate from fluvial networks [*Beaulieu et al.*, 2011], which therefore play a relevant role in greenhouse gas emissions, provided that the overall warming capacity of $N_2O$ is 300 times higher than that of $CO_2$ [*Intergovernmental Panel on Climate Change*, 2007; *Beaulieu et al.*, 2008; *Mulholland et al.*, 2008; *Beaulieu et al.*, 2009, 2011; *Syakila and Kroeze*, 2012; *Rosamond et al.*, 2012].

Fluvial networks, which link landscapes to the atmosphere and the oceans, are spatially extensive, with a structure optimized to minimize energy expenditure of the hydrological fluxes [*Rinaldo et al.*, 1993]. Streams and their associated surface and subsurface habitats, which include riparian areas and subsurface hyporheic zones, receive reactive inorganic N species, primarily as dissolved nitrate ($NO_3^-$) and ammonium ($NH_4^+$), from overland flows, groundwater contributions, and atmospheric deposition [*Peterson et al.*, 2001; *Beaulieu et al.*, 2011]. In streams, the hyporheic zone, which is the interface beneath and alongside a streambed where shallow groundwater and surface water mix, plays a key role in the biological transformation of inorganic N due to the longer residence time of water, compared to shorter retention within surface storage zones. As streamflow transports inorganic N to oceans, microbially mediated denitrification converts a proportion of the nitrate load into $N_2O$ and dinitrogen gas ($N_2$) [*Kroeze and Seitzinger*, 1998].

Until recently, rates and drivers of denitrification in streams were understudied, which motivated the second Lotic Intersite Nitrogen eXperiment (LINXII) [*Mulholland et al.*, 2008; *Beaulieu et al.*, 2011], whose primary objective was to quantify rates and controls on nitrate-N removal, including $N_2O$ emissions, from 72

headwater streams draining three different land use types (reference, agricultural, and urban) distributed across nine different U.S. biomes [*Beaulieu et al.*, 2011]. The LINXII streams were generally small, with stream discharges at baseflow conditions ranging from <1 to 268 L $s^{-1}$, while streambed morphology was diverse and included dunes, pool-riffles, plane beds, step pools, and cascade [*Mulholland et al.*, 2008; *Beaulieu et al.*, 2011]. Land use adjacent to, and within 1 km upstream of each study reach, was used to define the stream as being dominated by reference (native vegetation), urban or agricultural land uses. The predominance of each land use type was associated with varying total Dissolved Inorganic Nitrogen loads $DIN_0$, given by the sum of the concentrations of $NO_3^-$ and $NH_4^+$ in the stream water with $NO_3^-$ concentrations chiefly controlling the variations of DIN loads observed in the LINXII sites [*Mulholland et al.*, 2008, 2009]. For example, average $DIN_0$ was highest in agricultural catchments ($DIN_0 = 1328$ μ g N $L^{-1}$), followed by urban ($DIN_0 = 588$ μ g N $L^{-1}$) and then reference catchments ($DIN_0 = 113$ μ g N $L^{-1}$). Measurements from the LINXII study of stream $N_2O$ production via direct denitrification [*Beaulieu et al.*, 2011], and $N_2O$ emission rates to the atmosphere, demonstrated that $N_2O$ gas production was significant. The reaction was presumed to occur within streambed sediments as indirect denitrification, represented as denitrification of $NO_3^-$ within hyporheic sediments or from inputs of $N_2O$ from groundwater [*Beaulieu et al.*, 2011]. The latter contribution was shown to be negligible in the LINXII streams, as was the process of ANaerobic AMMonium OXidation [*Beaulieu et al.*, 2011], which converts ammonium directly to nitrogen gases under anaerobic conditions. Therefore, we must assume that the indirect denitrification responsible for the majority of $N_2O$ gas production quantified in the LINXII measurements was primarily occurring within the hyporheic zone.

The LINXII study used 24 h $^{15}NO_3$ tracer additions to quantify transformation rates, thus the microbially mediated transformations of $NO_3^-$ occurring within stream sediments (e.g., denitrification) had to depend on $NO_3^-$ delivered from the stream water to the sediments, along with the residence time of the associated pore water flux within the streambed itself. Owing to the short duration of the experiments, LINXII measurements do not characterize coupled nitrification-denitrification; therefore, they are in principle conservative estimates of $N_2O$ production via denitrification. Although no LINXII study directly demonstrated that denitrification occurred within the hyporheic zone, a similar in-stream injection experiment with simultaneous subsurface sampling showed that hyporheic zone denitrification in shallow flow paths (<4 cm below the streambed) could explain whole-stream reactions [*Harvey et al.*, 2013]. In addition, the hyporheic residence time, which is the time stream water spends in the streambed sediments, has been shown to be an important controlling factor of N transformations within the hyporheic zone [*Marzadri et al.*, 2011; *Zarnetske et al.*, 2011; *Gomez et al.*, 2012; *Marzadri et al.*, 2012; *Zarnetske et al.*, 2012; *Harvey et al.*, 2013]. Given these considerations, we argue that in addition to microbial denitrifiers colonizing streambed sediments, the hydromorphologic signature specific to each stream determines the proportion of $N_2O$ production due to indirect denitrification. To address our hypothesis, we interpret the LINXII data via a new upscaling methodology, which uses only reach-scale field measurements and hydromorphologic relationships to characterize biogeochemical and hydraulic conditions of streams and their hyporheic zones. We show the signature of both biogeochemical reactions and river morphology on stream solute transformations by normalizing the reaction products and key processes by suitable scaling factors.

## 2. Methods

Using the LINXII data, we show that the combined effect of hydromorphologic and biogeochemical characteristics of streams on $N_2O$ emissions can be encapsulated using a biogeochemical Damköhler number, which we define as

$$Da = \tau_{50}/\tau_{\mathrm{lim}} \tag{1}$$

where $\tau_{50}$ is the median residence time of stream water within the streambed sediment and $\tau_{lim}$ is a characteristic time of the biogeochemical reaction. $\tau_{50}$ represents the time at which 50% of water which crossed the downwelling area at time $t = 0$ is still within the hyporheic zone. In a previous study, we introduced this dimensionless number to investigate the control of stream morphology, streamflow, water temperature, and biogeochemical reaction rates on prevailing aerobic or anaerobic conditions within the hyporheic zone [*Marzadri et al.*, 2012]. A similar index has also been applied in other works to investigate nitrogen cycles [*Gomez et al.*, 2012; *Zarnetske et al.*, 2012; *Harvey et al.*, 2013]. Our approach is based on the premise that the potential for developing anaerobic conditions within the hyporheic zone, as described by *Da*, can serve as a surrogate for $N_2O$ production, because denitrification primarily occurs in anaerobic

zones. Since half of the water returning to the stream through the upwelling area remained within the hyporheic zone longer than $\tau_{50}$, prevailing anaerobic or aerobic conditions occur within the hyporheic zone when *Da* is larger or smaller than 1. The Damköhler number increases with water residence time and/or as a result of rapid dissolved oxygen consumption, as would occur due to elevated heterotrophic respiration within streambed sediments. Therefore, we hypothesize that $N_2O$ emissions will increase with increasing *Da* because anaerobic conditions are most favorable for denitrification. In the present work, we did not consider emissions of $N_2$ through complete denitrification because LINXII data do not provide such information.

To test the relationship between *Da* and $N_2O$ emission rates, we analyzed the data of the subset of LINXII streams for which information on morphologic [*Mulholland et al.*, 2008], hydraulic [*Mulholland et al.*, 2008], and biologic [*Beaulieu et al.*, 2011] parameters were sufficient to quantify *Da*.

### 2.1. Characterization of Stream Morphology and Evaluation of $\tau_{50}$

In steady state flow conditions, the residence time distribution within the hyporheic zone is chiefly controlled by river morphology, which influences the variety of pathways that a solute molecule could follow within the alluvium, depending on its entry point in the downwelling area [*Elliott and Brooks*, 1997; *Packman and Bencala*, 2000; *Haggerty et al.*, 2002; *Cardenas et al.*, 2004; *Boano et al.*, 2007; *Tonina and Buffington*, 2009a; *Stonedahl et al.*, 2010]. We characterize the residence time through the median residence time $\tau_{50}$ associated to the dominant river morphology, thereby assuming that streambed features at larger or smaller scales than the dominant topography have secondary effects on hyporheic processes at the reach scale [e.g., *Tonina and Buffington*, 2009b]. Here we use field data and available hydromorphological relationships for pool-riffle and dune morphologies at the reach scale to quantify $\tau_{50}$ and $\tau_{\text{lim}}$.

For the LINXII streams, the following quantities were independently measured [*Mulholland et al.*, 2008]: water discharge ($Q$), mean flow velocity ($V$), stream width ($W$), median grain size of the streambed sediment ($d_{50}$), and mean reach bed slope ($s_0$). The mean flow depth was estimated as follows: $Y_0 = Q/(W\,V)$.

We classify the streambed morphology and select the hyporheic model according to $s_0$, $d_{50}$, and field inspection. In particular, reaches with $s_0 < 0.009$ and $d_{50} < 4$ mm are classified as dune, those with $0.009 < s_0 < 0.05$ and $d_{50} > 4$ mm as pool-riffle [*Montgomery and Buffington*, 1997], while reaches with $s_0 > 0.05$ and $d_{50} > 4$ mm are classified as step-pool or cascade. This characterization was supported by field inspection of the LINXII streams. At present, there are no hyporheic models available for streams with step-pool and cascade morphologies; thus, as a first approximation, we apply to them the pool-riffle hyporheic model [*Hester and Doyle*, 2008; *Endreny et al.*, 2011; *Hassan et al.*, 2014]. We set the thickness of the alluvium depth so that it does not constrain the hyporheic flow, the porosity to $\phi = 0.32$, and the hydraulic conductivity, which is assumed homogeneous and isotropic, is computed with the following empirical relationship $K_H = 16.88 + 10.6\,d_{50}$, (where $K_H$ is in m d$^{-1}$ and $d_{50}$ is in mm) [*Salarashayeri and Siosemarde*, 2012]. Since the bed form wavelength and amplitude were not available, we used the theoretical hydromorphological relationships described below to derive their values from the available hydraulic and morphological information.

For streams with dune morphology, $\tau_{50}$ is quantified by means of the hyporheic model proposed and validated by *Elliott and Brooks* [1997] [see also *Packman and Bencala*, 2000; *Marion et al.*, 2002]:

$$\tau_{50} = \frac{\tau_{50}^*}{\lambda^2\, h_m\, K_H} \tag{2}$$

where $\tau_{50}^*$ is the dimensionless median hyporheic residence time, which assumes the following expression: $\tau_{50}^* = 4\,\phi\cos^{-1}(0.5)$, with $\cos^{-1}(\cdot)$ indicating the arc cosine of the argument. Furthermore, in equation (2), $\lambda = 2\,\pi/L$, with $L$ being the bed form length, is the bed form wavelength and $h_m$ is the amplitude of head variation, which depends on stream hydrodynamic parameters through the following expression proposed by *Shen et al.* [1990]:

$$h_m = \frac{0.28\,V^2}{2\,g}\begin{cases}\left(\frac{H_d}{0.34\,Y_0}\right)^{3/8} & \text{if } \frac{H_d}{Y_0} < 0.34,\\ \left(\frac{H_d}{0.34\,Y_0}\right)^{3/2} & \text{if } \frac{H_d}{Y_0} > 0.34.\end{cases} \tag{3}$$

where $g$ is the gravitational acceleration and $H_d$ is the bed form height. Finally, the values of $H_d$ and $L$ are computed using the empirical relationship proposed by *Yalin* [1964]: $H_d = 0.167\,Y_0$ and $L = 6\,Y_0$.

For streams with pool-riffle, $\tau_{50}$ is quantified with the approach proposed and validated by *Marzadri et al.* [2012]:

$$\tau_{50} = \frac{\tau_{50}^{*} L}{C_z s_0 K_H} \tag{4}$$

where $C_z$ is the dimensionless Chezy coefficient, quantifying streambed resistance and $L = 6W$ is the bar length. The dimensionless median residence time $\tau_{50}^{*}$ can be estimated with the following exponential function for fully submerged alternate bar topography [*Marzadri et al.*, 2012]:

$$\tau_{50}^{*} = 0.21 \exp(1.22 Y_D^{*}) \tag{5}$$

where $Y_D^{*}$ is the dimensionless streamflow depth ($Y_D^{*} = Y_0/H_d$) with respect to $H_d$, which is given by the following expression provided by *Ikeda* [1984]:

$$H_d = Y_0 \left(0.18\, d_s^{0.45}\, \beta^{1.45}\right) \text{ for } 2 < \beta < 35 \tag{6}$$

where $\beta = W/(2Y_0)$ is the alternate bar aspect ratio and $d_s = d_{50}/Y_0$ is the relative submergence.

Equations (2) and (4) are obtained under steady state flow conditions in the stream and the hyporheic zone underneath, while parameters describing streambed morphology have been obtained by assuming that the experiments were performed when water discharge was close to the formative water discharge. The last hypothesis is needed in order to obtain the bed form height $H_d$ from equation (6). Long-term morphological changes can be accommodated by changing $H_d$ and the water discharge while maintaining the hypothesis of steady state flow. As an alternative, $\tau_{50}$ may be determined by tracer experiments.

### 2.2. Characterization of Stream Biogeochemistry and Evaluation of $\tau_{lim}$

The residence time limit, $\tau_{lim}$, represents the time needed to consume the dissolved oxygen (DO) of the hyporheic water to a prescribed threshold ($DO_{lim}$) and can be defined as follows [*Marzadri et al.*, 2011]:

$$\tau_{lim} = \frac{1}{K_{R,t} + K_{N,t}} \ln\left(\frac{DO_0}{DO_{lim}}\right) \tag{7}$$

where $K_{R,t}(d^{-1})$ and $K_{N,t}(d^{-1})$ are the reaction rates of aerobic respiration and nitrification, respectively, $DO_0$ is the dissolved oxygen concentration of the stream water, and $DO_{lim}$ is set equal to the limit value for hypoxic conditions. In the present work, we assume $DO_{lim} = 2\ mg\ L^{-1}$, as suggested by *Rosamond et al.* [2012]. The reaction rate of aerobic respiration is obtained from the ecosystem respiration *ER*, while the reaction rate of nitrification is estimated on the basis of the areal rate of nitrification $U_{nit}$, through the following expressions adapted from *Mulholland et al.* [2002]:

$$K_{R,t} = \frac{ER}{Y_0 DO_0} \quad \text{and} \quad K_{N,t} = \frac{U_{nit}}{Y_0\, [NH_4^{+}]_0} \tag{8}$$

where the values of *ER* [g $O_2$ $m^{-2}$ $d^{-1}$] and $U_{nit}$ [μ g N $m^{-2}$ $d^{-1}$] were determined experimentally [*Mulholland et al.*, 2009]. Possible effects of land use on microbial activities are lumped into the reaction rates through equation (8) in our analysis. Land use may also affect streambed morphology, organic matter availability, and these could be partially accounted into the reaction rates and in the hydromorphologic parameters of the stream, such as discharge, mean flow velocity, and channel width.

### 2.3. Evaluation of $N_2O$ Flux Emitted From the Hyporheic Zone for Indirect Denitrification: $FN_2O_{HZ}$

For the LINXII streams, the $N_2O$ emitted to the atmosphere ($N_2O_{emission\ rate}$ (μ g N $m^{-2}$ $h^{-1}$)) is the sum of the $N_2O$ produced by direct denitrification in the stream and by indirect denitrification occurring within the hyporheic zone, as shown by *Beaulieu et al.* [2011]:

$$\underbrace{N_2O_{emission\ rate}}_{A} = \underbrace{N_2O_{direct\ denitrification}}_{B} + \underbrace{N_2O_{indirect\ denitrification}}_{C}, \tag{9}$$

and

$$N_2O_{emission\ rate} = k_2\, Y_0\, [N_2O]_{obs} - k_2\, Y_0\, [N_2O]_{eq} = FN_2O_{obs} - FN_2O_{eq} \tag{10}$$

where $k_2$ is the empirically measured air-water gas exchange rate ($h^{-1}$) [*Beaulieu et al.*, 2011], $[N_2O]_{obs}$ and $[N_2O]_{eq}$ are the measured concentrations of dissolved $N_2O$($\mu g\, N\, L^{-1}$) in the stream water and the dissolved $N_2O$ concentration ($\mu g\, N\, L^{-1}$) expected if the stream was in equilibrium with the atmosphere, respectively [*Beaulieu et al.*, 2011]. Finally, $FN_2O_{obs}$($\mu g\, N\, m^{-2}\, h^{-1}$) and $FN_2O_{eq}$($\mu g\, N\, m^{-2}\, h^{-1}$) are the corresponding measured and expected $N_2O$ fluxes. According to the Henry's law, and under the hypothesis of stream water with low salinity, $[N2O]_{eq}$ can be evaluated as follows [*Weiss and Price*, 1980]:

$$[N_2O]_{eq} = \left[p_{N_2O} \exp\left(A_1 + A_2 \frac{100}{T} + A_3 \ln\left(\frac{T}{100}\right)\right)\right] \frac{MW}{0.31824} 10^6 \tag{11}$$

where $A_i (i = 1, 2, 3)$ are constants [*Weiss and Price*, 1980], $T$ is the water temperature (°K), $p_{N_2O}$ is the partial pressure of $N_2O$ in the air (atm), and $MW$ is the molecular weight of N. For the LINXII data we assume that $p_{N_2O} = 315$ ppbv $= 315 \times 10^{-9}$atm [*Beaulieu et al.*, 2011]. Under these assumptions, the flux of $N_2O$ emitted by the hyporheic zone for indirect denitrification is given by the following:

$$\begin{cases} N_2O_{\text{emission rate}} = FN_2O_{obs} - FN_2O_{eq} \\ FN_2O_{obs} = FN_2O_{stream} + FN_2O_{HZ} \\ FN_2O_{HZ} = N_2O_{\text{emission rate}} - FN_2O_{stream} + FN_2O_{eq} \end{cases} \tag{12}$$

To account for different inorganic N loads, which influence stream-specific $N_2O$ production rates, we define the dimensionless flux of $N_2O$, $FN_2O^*_{HZ}$, as the ratio between the $N_2O$ mass flux, $FN_2O_{HZ}$, and the total stream mass flux of $[NO_3^-]$ and $[NH_4^+]$, which are the potential sources of $N_2O$ [*Mulholland et al.*, 2009]:

$$FN_2O^*_{HZ} = \frac{FN_2O_{HZ}}{\left([NO_3^-] + [NH_4^+]\right) V} \tag{13}$$

## 3. Results

We find that the dimensionless flux of $N_2O$ emitted from the hyporheic zone as a result of indirect denitrification ($FN_2O^*_{HZ}$) does not depend on land use (Figure 1a, analysis of variance (ANOVA), $F = 1.409$ and $p = 0.265$). However, land use chiefly impacts $N_2O$ emissions through the control of N loads to streams. In other words, we showed by normalizing the products ($N_2O$ fluxes) by their reactants (DIN fluxes) that the amount of reactants is the primary effect of land use on $N_2O$ production. Consequently, LINXII data can be analyzed further without having to separate streams by land use.

We interpret the LINXII data by using the travel time models presented in section 2.1 for pool-riffle and dune geometries, which relate streamflow depth to the median hyporheic residence time [*Elliott and Brooks*, 1997; *Tonina and Buffington*, 2009a; *Marzadri et al.*, 2010, 2012]. This modeling approach allows us to characterize the hyporheic residence time, thereby avoiding a time consuming and costly detailed survey of the streambed topography, because all model parameters are derived from reach-scale global geomorphological characteristics and estimation of the reaction rates.

This analysis shows that $FN_2O^*_{HZ}$ is strongly related to the Damköhler number (Figure 1b) for all the modeled LINXII streams for which sufficient data were available. This confirms that for a given inorganic N flux in a stream, $N_2O$ production is proportional to the median residence time of water into the hyporheic zone, in turn dependent on stream hydromorphology, and inversely proportional to the reaction rate, as encapsulated in the *Da* number.

The relationship between *Da* and $FN_2O^*_{HZ}$ can be described with a statistically significant power law function of *Da* (Bravaris-Pearson correlation coefficient $r^2 = 0.53$, followed by $t$ test, $t_{calculated} = 5.208 > 1.711$, $p = <0.001$). We also found that $N_2O$ emissions from reference streams have a smaller range of variability around this regression function than those streams dominated by urban or agricultural land use, although both the interquartile and the 0.9 interquantile range are smaller for the urban streams (Figure 1a). These results suggest that hydromorphologic and biogeochemical signatures, combined with inorganic N loads, are the main drivers of $N_2O$ emissions from streams.

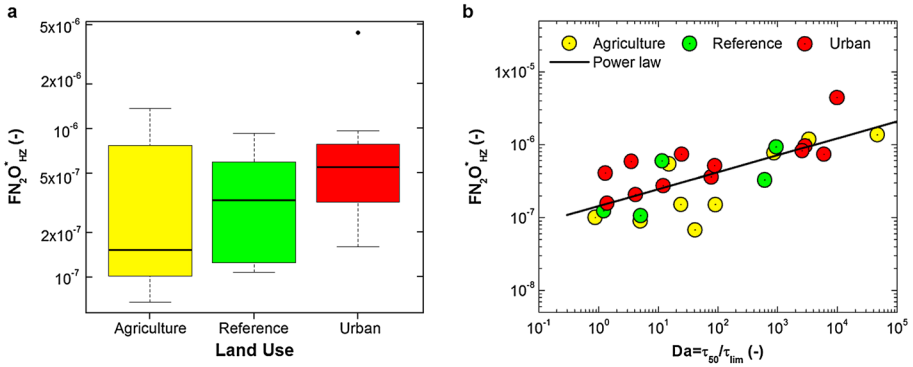


**Figure 1.** Effect of land use on $N_2O$ flux. (a) Box plot of $FN_2O^*_{HZ}$ grouped according to the prevalent land use of the catchment draining into the stream (agricultural, reference and urban); differences between land use types are not statistically significant (one-way ANOVA, F=1.409 and p=0.265). (b) Variation of the dimensionless flux of nitrous oxide $FN_2O^*_{HZ}$ as a function of the Damköhler number $Da = \tau_{50}/\tau_{lim}$. The best fit of the power law function with the data is also shown: $FN_2O^*_{HZ} = 1.410 \times 10^{-7} Da^{0.23}$ ($r^2 = 0.53$).

To further explore the role of stream morphology on watershed $N_2O$ emissions, we examine the LINXII data focusing on streams characterized by step-pool or cascade morphology ($n = 8$ reference, $n = 1$ urban streams). Our approach is to analyze these streams separately as if they were characterized by a hyporheic flow induced by pool-riffle morphology; in the absence of a specific model for steep-pool or cascade morphology, this is justified because in both bed forms the near-bed head profile is dominated by the hydrostatic head, rather than the dynamic head, as occurs for dunes [*Hester and Doyle*, 2008; *Tonina and Buffington*, 2009a; *Endreny et al.*, 2011; *Hassan et al.*, 2014]. In other words, from a hydrodynamic perspective, the functioning of step-pool or cascade morphology is more similar to pool-riffle than dune morphology. This assumption is supported by our finding that the dimensionless $N_2O$ emissions from streams with step-pool and cascade morphologies show a different functional dependence from *Da* than the data for pool-riffle and dune morphology (Figure 2, analysis of covariance (ANCOVA), $F = 10.04$, $p < 0.01$). Again, we find that the dependence of the dimensionless $N_2O$ emissions on stream hydromorphology and biogeochemistry can be encapsulated by *Da*, which then allows to estimate $N_2O$ emissions using reach-scale hydromorphological characteristics and inorganic N concentrations. In addition, our model provides a reliable and physically based tool to effectively upscale processes from bed form scale to the reach and larger scales, provided that morphological and geochemical information is available. It represents an effective methodology to fill the knowledge gap recognized among others by *Gariner et al.* [2009] and *Beaulieu et al.* [2011] on the ability to estimate $N_2O$ emissions from indirect denitrification from river water variables (e.g., DO and DIN) and river morphology.

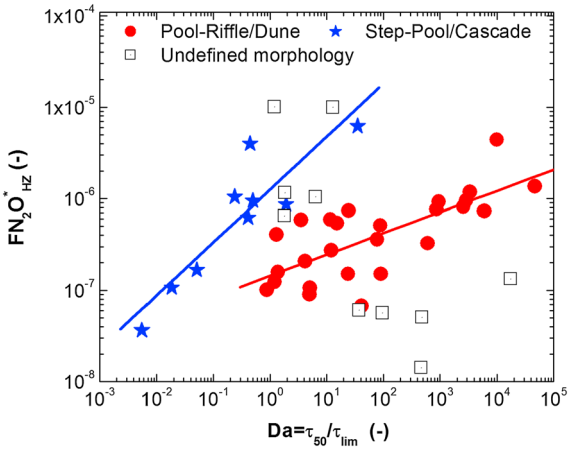


**Figure 2.** Effect of stream morphology on $N_2O$ flux. Dimensionless flux of nitrous oxide $FN_2O^*_{HZ}$ as a function of the Damköhler number $Da = \tau_{50}/\tau_{\mathrm{lim}}$ separately for two groups of morphologies: pool-riffle or dune and step-pool or cascade. The blue solid line is the best fit of the power law function with the data for streams with step-pool/cascade morphology $FN_2O^*_{HZ} = 1.2 \times 10^{-6} Da^{0.58}$ ($r^2 = 0.81$), which differs significantly (ANCOVA, $F = 10.04$ and $p < 0.01$) from the best fit of the power law function with the data for streams with pool-riffle/dune morphology: $FN_2O^*_{HZ} = 1.4 \times 10^{-7} Da^{0.22}$ ($r^2 = 0.53$) represented in the graph with the red line. The dimensionless $N_2O$ emissions from 11 streams for which the morphology is undefined are also shown (open boxes).

Morphological classification of a stream is therefore a prerequisite for using *Da* as a predictor of $N_2O$ emissions; without hydromorphologic information, we find that predictions of $N_2O$ emissions from streams is much more uncertain. This is evidenced by the large scatter of the undefined streams,

shown with open boxes in Figure 2, which are modeled as dune or pool-riffle according to the classification proposed in section 2. These cases include streams whose morphology could not be defined or does not lead to a significant hyporheic exchange.

Our results suggest that the quantification of *Da*, via the dominant geomorphologic feature, sediment properties, and biogeochemical activity captures the first-order controls on nitrogen transformation. All parameters used to quantify *Da* are taken from field measurements, field evidences, or derived from field data via appropriate relationships and none is calibrated. For instance, the hydraulic conductivity is obtained from a relationship with $d_{50}$, which is measured from samples taken in the field during the LINXII experiments. This relationship is affected by uncertainty as all empirical relationships but it captures the order of magnitude of the sediment properties as derived from texture data. Similarly, $\tau_{50}$ induced by the dominant topography provides the order of magnitude of the characteristic hyporheic residence time. Consequently, part of the scatter around the trend in Figure 1b could be due to hyporheic exchange induced by other interactions, uncertainty of streambed hydraulic conductivity, and field measurement error. All these uncertainties notwithstanding, the analysis shows the clear fingerprint of *Da* over about five log scales, which is well beyond what can be a reasonable quantification of uncertainty. Additionally, the model results were also robust and fell in the same trend as those of Figure 1b by changing $\pm 30\%$ the value of the mean flow depth, a key morphological parameter, which is used in the definition of both $\tau_{50}$ and $\tau_{\text{lim}}$. The residence time, in fact, varies according to the point where the particle (solute molecule) enters the hyporheic zone through the downwelling area. Consequently, *Da* captures in a single parameter the effect of river morphology, hydraulic conductivity of the alluvium, and biogeochemical characteristics. Since the data for both morphologies fall on the same dimensionless trend in Figure 2, we conclude that the model captures the main processes leading to denitrification and $N_2O$ emissions in a wide range of streams, such as those considered in the LINXII experiment. Similarly, the fact that step-pool and cascade-induced hyporheic processes define a different trendline, as confirmed by the ANCOVA test, suggests that pool-riffle hyporheic model does not correctly represent that morphology but rather scales it. We hypothesize that an analysis of the step-pool/cascade data with the appropriate hyporheic model, once available, should collapse all data along one single trend. Although the LINXII data set showed that land use chiefly controls $N_2O$ emissions by affecting reactants loads, DIN, other effects of land use, on organic matter availability and on river morphology could potentially control $N_2O$ emissions. Our method could implicitly account for these land use effects, when present, implicitly through both $\tau_{50}$ and $\tau_{\text{lim}}$.

## 4. Conclusions

We show that $N_2O$ emissions from rivers can be expressed as a power law function of the Damköhler number *Da*, given by the ratio between the median residence time of water into the hyporheic zone and a characteristic time of the geochemical transformation. All parameters used to quantify *Da* are reach-scale values capturing the general geomorphologic characteristics of the streambed, sediment properties, and biogeochemical activity and are taken from field measurements, field evidences, or derived from field data via appropriate relationships, thereby suggesting a possible way to upscale emissions from the reach to the river network scale. Using the LINXII data, we demonstrate the functional dependence of $N_2O$ flux on *Da* and underscore the importance of stream morphology when interpreting experimental results and upscaling $N_2O$ emissions from the reach to the network scale. Our findings also show that the main effect of land use is on the nitrogen load, whereas its impact, which we account for in our modeling approach through $\tau_{\text{lim}}$, on the processes leading to nitrogen transformation and $N_2O$ emission is not statistically significant in the LINXII study sites.

**Acknowledgments**

This research is partially supported by the Deadwood River Project, U.S. Forest Service award 009421-01 and by the Italian Ministry of Public Instruction, University and Research through the project PRIN 2010-2011, protocol 2010JHF437: "Innovative methods for water resources management under hydroclimatic uncertainty scenarios." We also thank the LINXII group for providing empirical data that supported the development of the model described in this manuscript (http://www.faculty.biol.vt.edu/webster/linx/).

The Editor thanks two anonymous reviewers for their assistance in evaluating this paper.

## References

Alexander, R. B., R. A. Smith, and G. E. Schwarz (2000), Effect of stream channel on the delivery of nitrogen to the Gulf of Mexico, *Nature*, *403*, 758–761.

Beaulieu, J. J., C. P. Arango, S. K. Hamilton, and J. L. Tank (2008), The production and emission of nitrous oxide from headwater in the Midwestern United States, *Global Change Biol.*, *14*, 878–894.

Beaulieu, J. J., C. P. Arango, and J. L. Tank (2009), The effects of season and agriculture on nitrous oxide production in headwater streams, *J. Environ. Qual.*, *38*, 637–646.

Beaulieu, J. J., et al. (2011), Nitrous oxide emission from denitrification in stream and river networks, *Proc. Natl. Acad. Sci. U.S.A.*, *108*(1), 214–219.

Boano, F., R. Revelli, and L. Ridolfi (2007), Bedform induced hyporheic exchange with unsteady flows, *Adv. Water Resour.*, *30*(1), 148–156.

Cardenas, M. B., J. L. Wilson, and V. A. Zlotnik (2004), Impact of heterogeneity, bed forms, and stream curvature on subchannel hyporheic exchange, *Water Resour. Res.*, *40*, W08307, doi:10.1029/2004WR003008.
Elliott, A. H., and N. H. Brooks (1997), Transfer of nonsorbing solutes to a streambed with bedforms: Theory, *Water Resour. Res.*, *33*, 123–136.
Endreny, T. A., L. Lautz, and D. Spiegel (2011), Hyporheic flow path response to hydraulic jumps at river steps: Hydrostatic model simulations, *Water Resour. Res.*, *47*, W02518, doi:10.1029/2010WR010014.
Galloway, J. N., J. D. Aber, J. W. Erisman, S. P. Seitzinger, R. W. Howarth, E. B. Cowling, and B. J. Cosby (2003), The nitrogen cascade, *BioScience*, *53*(4), 341–356.
Galloway, J. N., et al. (2004), Nitrogen cycles: Past, present, and future, *Biogeochemistry*, *70*, 153–226.
Gariner, J., J. Billen, G. Vilain, A. Martinez, M. Silvestre, E. Mounier, and F. Toche (2009), Nitrous oxide ($N_2O$) in the Seine river and basin: Observations and budgets, *Agric. Ecosyst. Environ.*, *133*, 223–233.
Gomez, J. D., J. L. Wilson, and M. B. Cardenas (2012), Residence time distributions in sinuosity-driven hyporheic zones and their biogeochemical effects, *Water Resour. Res.*, *48*, W09533, doi:10.1029/2012WR012180.
Haggerty, R., S. M. Wondzell, and M. A. Johnson (2002), Power-law residence time distribution in the hyporheic zone of a 2nd-order mountain stream, *Geophys. Res. Lett.*, *29*(13), 1640, doi:10.1029/2002GL014743.
Harvey, J. W., J. K. Böhlke, M. A. Voytek, D. Scott, and C. R. Tobias (2013), Hyporheic zone denitrification: Controls on effective reaction depth and contribution to whole-stream mass balance, *Water Resour. Res.*, *49*, 6298–6316, doi:10.1002/wrcr.20492.
Hassan, M. A., D. Tonina, R. D. Beckie, and M. Kinnear (2014), The effects of discharge and slope on hyporheic flow in step-pool morphologies, *Hydrol. Processes*, doi:10.1002/hyp.10155.
Hester, E. T., and W. A. Doyle (2008), In-stream geomorphic structures as drivers of hyporheic exchange, *Water Resour. Res.*, *44*, W03417, doi:10.1029/2006WR005810.
Ikeda, S. (1984), Prediction of alternate bar wavelength and height, *J. Hydraul. Eng.*, *110*(4), 371–386.
Intergovernmental Panel on Climate Change (2007), *Climate Change 2007: The Physical Science Basis*, Cambridge Univ. Press, Cambridge, U. K.
Kroeze, C., A. Moiser, and L. Bouwman (1999), Closing the global $N_2O$ budget: A retrospective analysis 1500–1994, *Global Biogeochem. Cycles*, *13*(1), 1–8.
Kroeze, K., and S. Seitzinger (1998), Nitrogen inputs to rivers, estuaries, continental shelves and related nitrous oxide emissions in 1990 and 2050: A global model, *Nutr. Cycling Agroecosyst.*, *52*, 195–212.
Marion, A., M. Bellinello, I. Guymer, and A. I. Packman (2002), Effect of bed form geometry on the penetration of nonreactive solutes into a streambed, *Water Resour. Res.*, *38*(10), 1209, doi:10.1029/2001WR000264.
Marzadri, A., D. Tonina, A. Bellin, G. Vignoli, and M. Tubino (2010), Semi-analytical analysis of hyporheic flow induced by alternate bars, *Water Resour. Res.*, *46*, W07531, doi:10.1029/2009WR008285.
Marzadri, A., D. Tonina, and A. Bellin (2011), A semianalytical three-dimensional process-based model for hyporheic nitrogen dynamics in gravel bed rivers, *Water Resour. Res.*, *47*, W11518, doi:10.1029/2011WR010583.
Marzadri, A., D. Tonina, and A. Bellin (2012), Morphodynamic controls on redox conditions and on nitrogen dynamics within the hyporheic zone: Application to gravel bed rivers with alternate-bar morphology, *Global Biogeochem. Cycles*, *117*, G00N10, doi:10.1029/2012JG001966.
Montgomery, D. R., and J. M. Buffington (1997), Channel-reach morphology in mountain drainage basins, *Geol. Soc. Am. Bull.*, *109*(5), 596–611.
Mulholland, P. J., et al. (2002), Can uptake length in streams be determined by nutrient addition experiments? Results from an interbiome comparison study, *J. N. Am. Benthol. Soc.*, *21*(4), 544–560.
Mulholland, P. J., et al. (2008), Stream denitrification across biomes and its response to anthropogenic nitrate loading, *Nature*, *452*, 202–206.
Mulholland, P. J., et al. (2009), Nitrate removal in stream ecosystems measured $^{15}N$ addition experiments: Nitrification, *Limnol. Oceanogr.*, *54*(3), 666–680.
Packman, A. I., and K. E. Bencala (2000), Modeling surface-subsurface hydrological interactions, in *Streams and Ground Waters*, edited by J. B. Jones and P. J. Mulholland, pp. 45–80, Academic Press, San Diego, Calif.
Peterson, B., et al. (2001), Control of nitrogen export from watershed by headwater streams, *Nature*, *292*, 86–89.
Rinaldo, A., I. Rodriguez-Iturbe, R. Rigon, E. Ijjasz-Vasquez, and R. L. Bras (1993), Self-organized fractal river networks, *Phys. Rev. Lett.*, *70*(6), 822–825.
Rosamond, M. S., S. J. Thuss, and S. L. Schiff (2012), Dependence on riverine nitrous oxide emissions on dissolved oxygen levels, *Nat. Geosci.*, *5*, 715–718.
Salarashayeri, A. F., and M. Siosemarde (2012), Prediction of soil hydraulic conductivity from particle-size distribution, *World Acad. Sci. Eng. Technol.*, *61*, 454–458.
Shen, H. V., H. M. Fehlman, and C. Mendoza (1990), Bed form resistances in open channel flows, *J. Hydraul. Eng.*, *116*(6), 799–815.
Stonedahl, S. H., J. W. Harvey, A. Wörman, M. Salehin, and A. I. Packman (2010), A multiscale model for integrating hyporheic exchange from ripples to meanders, *Water Resour. Res.*, *46*, W12539, doi:10.1029/2009WR008865.
Syakila, A., and C. Kroeze (2012), The global nitrous oxide budget revisited, *Greenhouse Gas Meas. Manage.*, *1*(1), 17–26.
Tonina, D., and J. M. Buffington (2009a), Hyporheic exchange in mountain rivers I: Mechanics and environmental effects, *Geography Compass*, *3*(3), 1063–1086.
Tonina, D., and J. M. Buffington (2009b), A three-dimensional model for analyzing the effects of salmon redds on hyporheic exchange and egg pocket habitat, *Can. J. Fish. Aquat. Sci.*, *66*, 2157–2173.
Vitousek, P. M., J. D. Aber, R. W. Howarth, G. E. Likens, P. A. Matson, D. W. Schindler, W. H. Schlesinger, and D. G. Tilman (1997), Human alterations of the global nitrogen cycle: Sources and consequences, *Ecol. Appl.*, *7*(3), 737–750.
Weiss, R. F., and B. A. Price (1980), Nitrous oxide solubility in water and seawater, *Mar. Chem.*, *8*, 347–359.
Yalin, M. S. (1964), Geometrical properties of sand waves, *J. Hydraul. Div.-ASCE*, *90*(5), 105–119.
Zarnetske, J. P., R. Haggerty, S. M. Wondzell, and M. A. Baker (2011), Dynamics of nitrate production and removal as a function of residence time in the hyporheic zone, *J. Geophys. Res.*, *116*, G01025, doi:10.1029/2010JG001356.
Zarnetske, J. P., R. Haggerty, S. M. Wondzell, V. A. Bokil, and R. González-Pinzón (2012), Coupled transport and reaction kinetics control on the nitrate sources-sink function of hyporheic zones, *Water Resour. Res.*, *48*(11), W11508, doi:10.1029/2012WR011894.